

ADAPTIVE SIGNAL PROCESSING FOR ADAPTIVE CONTROL

Bernard Widrow

Department of Electrical Engineering
Stanford University, Stanford, CA

Eugene Walach

Chaim Weitzman Postdoctoral Fellow, Department of Electrical Engineering
Stanford University, Stanford, CA

Abstract

A few of the well established methods of adaptive signal processing are modified and extended for application to adaptive control.

An unknown plant will track an input command signal if the plant is preceded by a controller whose transfer function approximates the inverse of the plant transfer function. An adaptive inverse modeling process can be used to obtain a stable controller, whether the plant is minimum or non-minimum phase. No direct feedback is involved. However the system output is monitored and utilized in order to adjust the parameters of the controller. The proposed method is a promising new approach to the design of adaptive control systems.

INTRODUCTION

There is a great need for learning-control systems which can adapt to the requirements of plants whose characteristics may be unknown and/or changeable in unknown ways. Two principal factors have hampered the development of adaptive controls, the difficulty of dealing with learning processes embedded in feedback loops, and the difficulty in controlling nonminimum-phase plants. Considerable progress has been made (see for instance works by Powell [9], Tse and Athans [10], Nakamura and Yoshida [8], Astrom and Wittenmark [2], [3], [4], Landau [5], [6], Martin-Sanchez [7]). However, interaction between the feedback of the learning process and that of the signal flow path still greatly complicates the analysis which is requisite to the design of dependable control systems.

In this paper we continue with the development of an alternative approach, which was first presented by B. Widrow and his students [14], [15], and B. D. O. Anderson [1], which circumvents many of the difficulties that have been encountered with the previous forms of adaptive control. The basic idea is to create a good transversal filter model of the plant, then to utilize it in order to obtain an inverse (or delayed inverse) of the plant. This inverse can be used as an open loop controller of the system. Since such a controller is realized as a transversal filter, the stability of the system is assured. Moreover it can be shown that, if one is willing to allow a delay in the response of the control

system, excellent control of the plant dynamics can be achieved, even for nonminimum phase plants.

ADAPTIVE FILTERING

A schematic representation of an adaptive filter is depicted in Fig. 1. The filter has an input u_j , an output

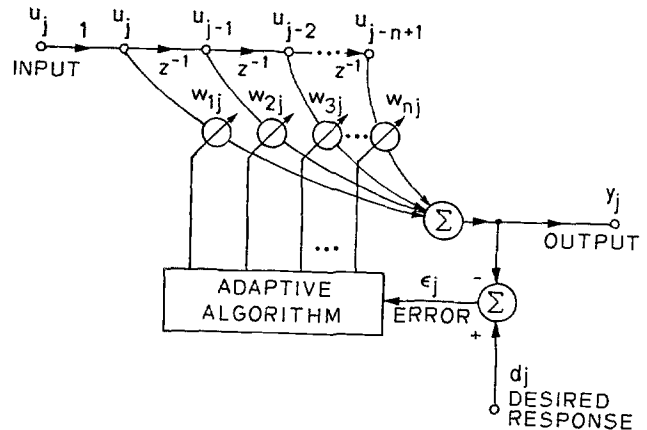


Fig. 1. An adaptive filter.

y_j , and it requires a special training signal called the "desired response" d_j . The error ϵ_j is the difference between the desired and actual output responses. The filter is assumed to be transversal and its weights w_{1j}, \dots, w_{nj} are adapted in order to minimize the expected square of the error ϵ_j . Various adaptation algorithms can be utilized for that purpose. Here we will employ the LMS steepest descent algorithm of Widrow and Hoff [11], [12], [13].

Consider the direct modeling of an unknown plant as shown in Fig. 2. When given the same input signal as that of an unknown plant, the adaptive model self-adjusts to cause its output to be a best least squares fit to the actual plant output. With a sufficient number of weights, an adaptive transversal filter can achieve a close fit to an unknown plant which may have many poles and zeros.

The inverse model of the unknown plant could be formed as shown in Fig. 3. The adaptive filter input is the plant output. The filter is adapted to cause its

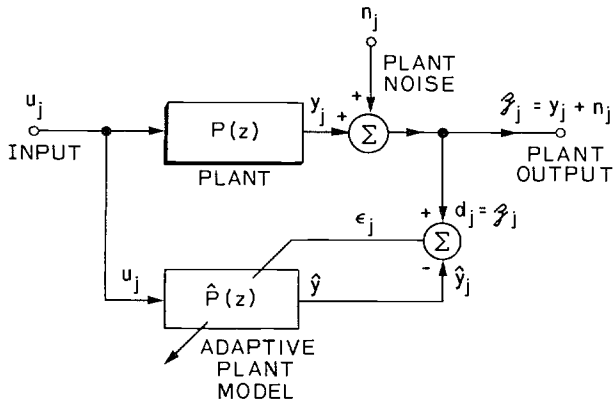


Fig. 2. Adaptive modeling.

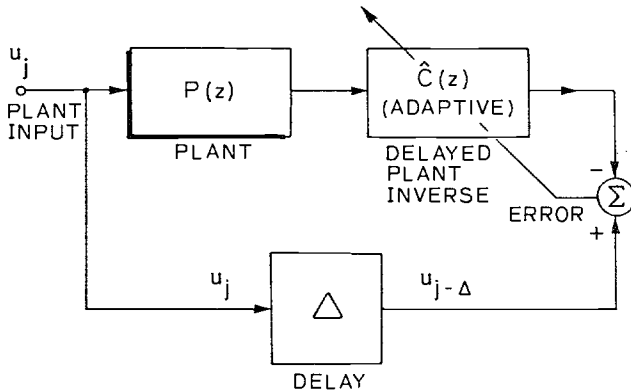


Fig. 3. Delayed inverse modeling.

output to be a best least squares fit to the plant input. A close fit implies that the cascade of the unknown plant and the LMS filter have a "transfer function" of essentially unit value.

If the plant itself is stable, all of its poles lie in the left half of the s -plane. But some of its zeros could lie in the right half plane, and then the plant would be nonminimum phase. The inverse of the minimum phase plant would have all of its poles in the left half plane, and there would be no problem with stability of the inverse. The non-minimum phase plant would have zeros in the right half plane and stability of the inverse would be an important issue. However, it can be shown that stable inverses for nonminimum phase plants could always be constructed if one were permitted noncausal two-sided impulse responses. Furthermore, with suitable time delays, causal approximations to delayed versions of noncausal impulse responses are realizable. Thus, by allowing a delay in the modeling process (as illustrated in Fig. 3), one can obtain approximate delayed inverse models to minimum phase and nonminimum phase plants. It is not necessary to know *a priori* whether the plant is or is not minimum phase. However, some

knowledge of plant characteristics would be helpful when choosing the delay Δ and the length of the transversal filter used for inverse modeling.

ADAPTIVE INVERSE CONTROL SCHEME

Using a stable delayed inverse, control is accomplished as illustrated in Fig. 4. The controller is a

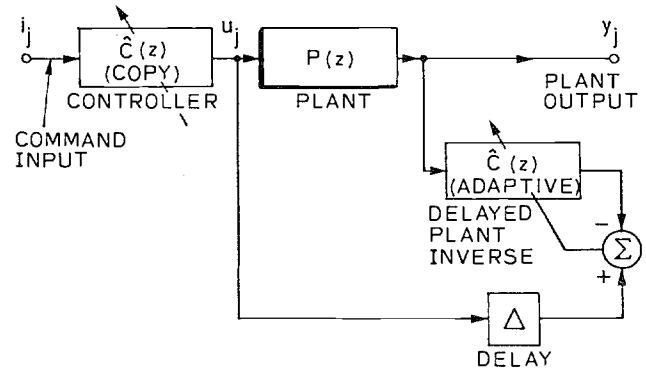


Fig. 4. An adaptive inverse control system.

copy of the inverse model. The command input i_j , the desired output for the plant, is applied as an input to the controller. The controller output is the driving function for the plant. If the controller were an exact delayed plant inverse, the plant output, assuming no noise, would be an exact copy of the input reference command, but delayed, i.e.,

$$y_j = i_{j-\Delta}$$

A step change in the command input would cause a step change in the plant output after a delay of Δ seconds. In order to illustrate this idea, computer simulations were performed. A nonminimum phase plant was controlled. Its impulse response is depicted in Fig. 5a. This stable underdamped plant has a small transport delay. In order to find the inverse, the scheme of Fig. 3 was used to adapt a transversal filter having 40 weights. Since the plant is nonminimum phase, a good (low error) causal inverse cannot be obtained. Hence for $\Delta=0$, the error power was close to the input power. However when the delay Δ was increased, the error power decreased indicating that very good plant inverses were obtained. Figure 5b shows the error power as a function of the modeling delay Δ . For $\Delta=26$, the error power decreased to below 5% of the input signal power. For this value of Δ , the best plant inverse had the impulse response shown in Fig. 5c. Connecting this as a controller in cascade with the plant, in the manner presented in Fig. 4, the overall impulse response was as shown in Fig. 5d. Clearly the behavior of the entire system closely approximated that of a pure delay. In Fig. 6b the step response of the control system is presented, and it may be compared to the ideal step response of Fig. 6a.

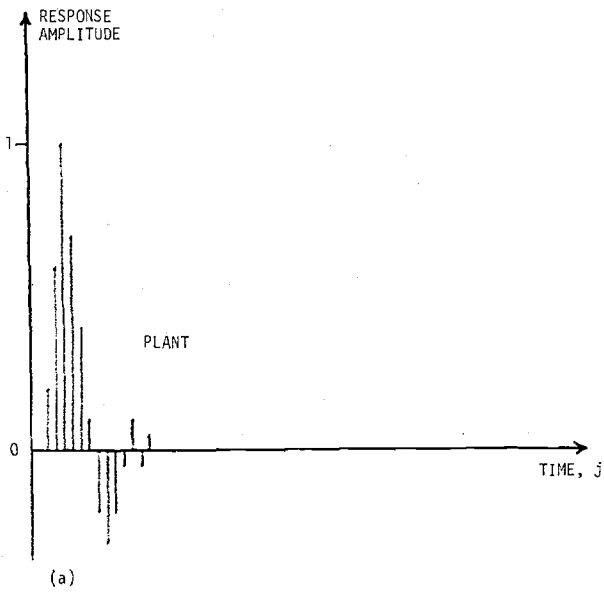


Fig. 5.

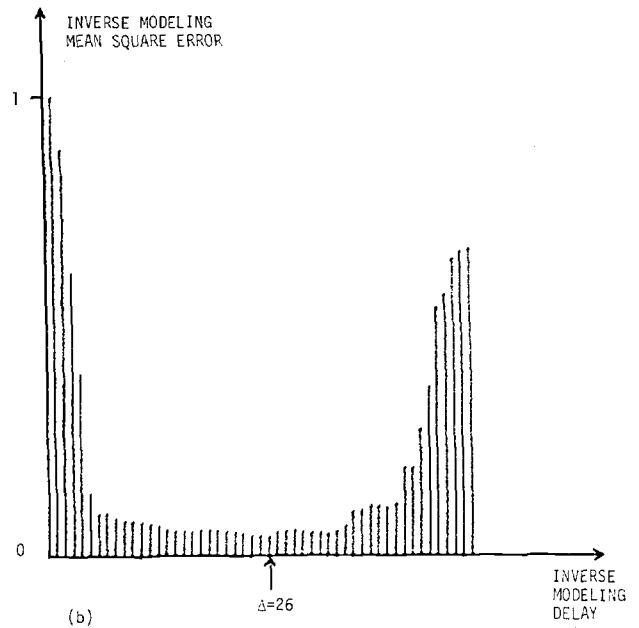


Fig. 5.

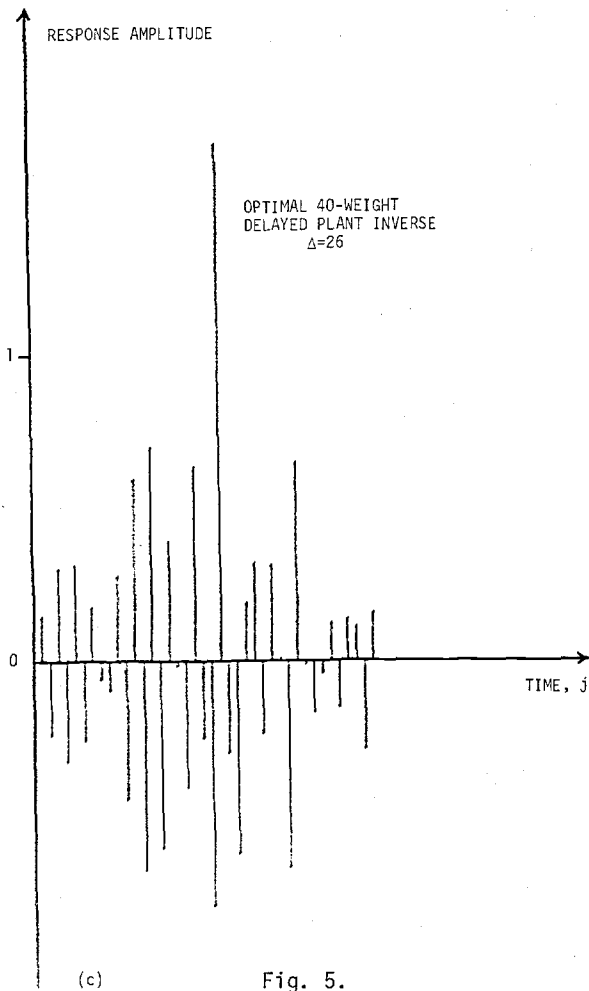


Fig. 5.

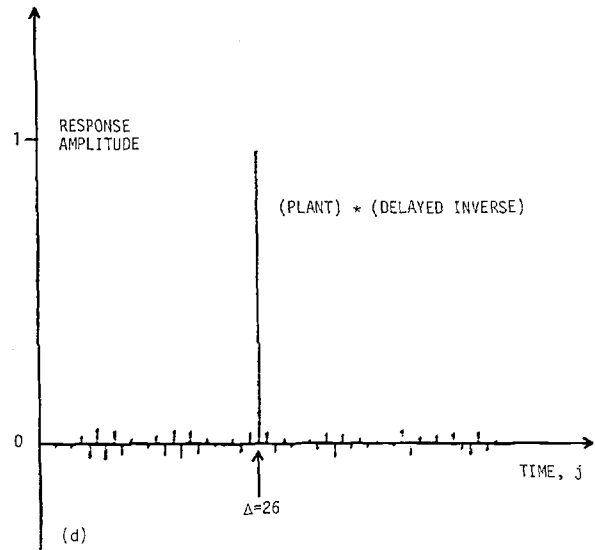


Fig. 5. Impulse response of plant and optimized 40-weight controller.

CONCLUSION

A method for adaptive inverse control has been introduced. The technique is easy to implement and exhibits robust, predictable behavior. Intensive research has been conducted in this area in order to enhance the potential capabilities of the proposed approach and to perform detailed analyses of the expected behavior. The results of this additional research are now being prepared for publication.

ADAPTIVE ALGORITHM

The coefficients a_n and b_n are adapted according to the well known steepest descent criteria for recursive and nonrecursive systems [1,2]. Using the block diagram in Fig. 1 together with the transfer function defined in Eqn. (1), we can write the following:

$$y_k = (1-r^2)[ax_{k-1}-x_{k-2}]+(1+r^2)ay_{k-1}-r^2y_{k-2} \quad (5)$$

$$\epsilon_k = x_k - y_k \quad (6)$$

$$y'_k = by_k \quad (7)$$

$$\epsilon'_k = x_k - y'_k \quad (8)$$

The subscripts denoting the stage number, n , have been omitted for notational simplicity. Due to the recursive nature of y_k , the desired partial derivative is also defined recursively as

$$\begin{aligned} \alpha_k &= \frac{\partial y_k}{\partial a} \\ &= (1-r^2)x_{k-1}+(1+r^2)[y_{k-1}+a\alpha_{k-1}]-r^2\alpha_{k-2} \end{aligned} \quad (9)$$

Using Eqns. (5-9) together with the steepest descent criteria, the adaptive coefficient updates are

$$a_{k+1} = a_k + \rho \epsilon_k \alpha_k \quad (10)$$

$$b_{k+1} = b_k + \mu \epsilon'_k y_k \quad (11)$$

where ρ and μ are constants which determine the rate of convergence. Note that at each iteration we are actually updating N sets of Eqns. (5-11).

EXPERIMENTAL RESULTS

Computer simulations were performed to demonstrate the performance of this ALE system for the previously described example. Initial conditions were selected to distribute three filter passbands in a comb pattern over the frequency range from 0 to $\pi/2$ radians. The resulting starting points were .26, .78, and 1.3 radians. The distribution with respect to the a_n performance surface is illustrated in Fig. 3. Note that the central point lies on an extremely flat portion of the surface, where gradient search algorithms are understandably inefficient.

The results of this experiment are presented in Fig. 4. The plots illustrate the magnitude of the gain coefficient, b_n , and the angle corresponding to the adaptive coefficient a_n for each of the three stages. Stage 1 quickly locked on to the incoming line at 0.4 radians, as would be expected from the initial conditions illustrated in Fig. 3.

Due to the flat surface, no signal was detected by stage 2. Note that the gain coefficient decays to zero as predicted. The line signal at 1.2 radians was detected by stage 3. Note the difference in rates of convergence from stage 1 to stage 3. This is consistent with the shape of the performance surface in Fig. 3, and suggests that a normalization factor based on the signal power might provide more uniform convergence characteristics.

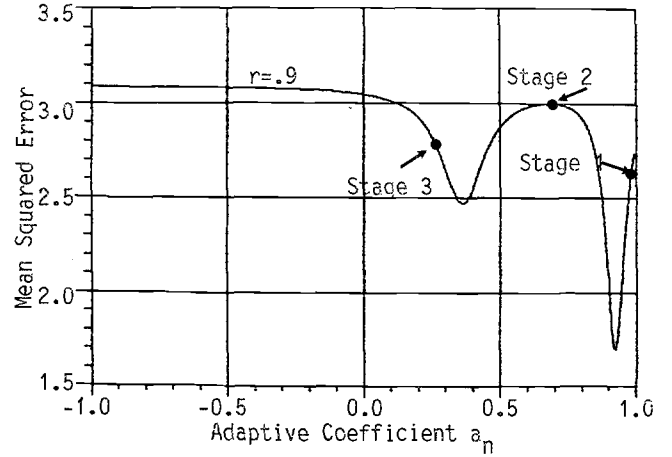
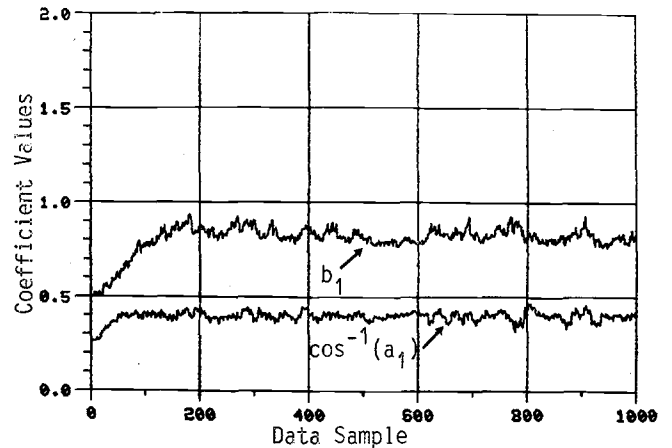


Figure 3. Initial Condition Distribution.



(a) Stage 1 Adaptive Coefficients

Figure 4. Experimental Results.